

A Novel Polyhedral Oligomeric Silsesquioxane-Cefotaxime Conjugate: Synthesis, Characterization, In Vitro Antibacterial Activity And Cellular Cytotoxicity

Idil Karaca Acari (Corresponding author)
Vahap Kucuk Vocational School, Malatya Turgut Ozal University
PO box 44210, Malatya, Turkey
E-mail: idil.karaca@ozal.edu.tr

Ismet Yilmaz
Department of Chemistry, Faculty of Science, Inonu University,
PO box 44280, Malatya, Turkey
E-mail: ismet.yilmaz@inonu.edu.tr

The research is financed by. Inonu University's scientific research projects unit (BAP) with code 2013/157.

Abstract

In recent years, polyhedral oligomeric silsesquioxanes (POSS) have become the subject of great interest. The main aim of this study is the development of a chloro-functionalized polyhedral oligomeric silsesquioxane (POSS-Cl) based novel polyhedral oligomeric silsesquioxane-cefotaxime (POSS-CTX) conjugate that exhibits potent antibacterial activity and biocompatibility. The chloro-functionalized POSS, cefotaxime (CTX) and polyhedral oligomeric silsesquioxane-cefotaxime (POSS-CTX) structures were characterized for their chemical structure, morphology and thermal behavior by employing fourier transform infrared spectroscopy (FTIR), ¹H nuclear magnetic resonance spectroscopy (NMR), scanning electron microscope/energy dispersive X-ray spectroscopy (SEM/EDX), and the thermal analysis differential thermal analyzer (DTA), thermo gravimetric analyzer (TGA), differential scanning calorimetric analyzer (DSC) techniques. In addition, the antibacterial activities were tested with broth microdilution methods on *E.coli* and *S.aureus* bacteria. The cellular cytotoxicity was performed on the L929 mouse skin fibroblast cell with MTT test. The IC₅₀ values of cefotaxime for *E.coli* and *S.aureus* were 62.71±14.30 and 144.17±20.90 µg/mL, respectively. However, in the POSS-cefotaxime (POSS-CTX) conjugate, the IC₅₀ values for *E.coli* and *S.aureus* were 11.51±3.02 and 26.20±11.14 µg/mL. These results suggest that the POSS-CTX conjugate was more antibacterial active than the cefotaxime. These POSS based antibacterial POSS-CTX conjugate can provide benefits many areas such as medical materials, antibacterial coating, antibacterial packaging.

Keywords: Polyhedral oligomeric silsesquioxane, Cefotaxime, Antibacterial Activities, Cellular Cytotoxicity.

1.Introduction

Polyhedral oligomeric silsesquioxanes have been the subject of great interest in many branches of materials chemistry. The general structure of POSS (RSiO_{3/2})₈ indicates the important features due to the siloxane cage size and the distribution of the eight pendant arms from the cube in a three dimensional arrangement (Cordes et al., 2010, Huang et al., 2013) The eight corners of the POSS cubic structure can be easily functionalized by connecting different groups (R, such as an alkyl, aryl, amine, imide, alcohol, thiol, olefin, and ester etc.) (Li et al., 2001, Li et al., 2009, Liang et al., 2005). Due to the bioavailability, chemical and thermal stability, POSS is suitable for using in medical fields such as the drug transport system, dental composites, biosensors, biomedical equipment, and tissue engineering (McCusker et al., 2005, Fong et al., 2005, Zou et al., 2007, Sarkar et al., 2009, Ghanbari et al., 2010). Cefotaxime is a drug of the third-generation cephalosporin antibiotic (Fakhri et al., 2016, Türkes et al., 2015). It shows a broad spectrum of antibacterial activity against clinically isolated strains of gram-negative and gram positive

bacteria (Masuyashi et al., 1980). This study aims to develop a novel POSS based POSS-CTX structural design. POSS-CTX conjugate was synthesized by condensation reaction. The prepared POSS-CTX structure was characterized for their structure, morphology, and thermal behavior by employing Fourier transform infrared spectroscopy, nuclear magnetic resonance spectroscopy, scanning electron micrograph, and thermal analysis (DTA/TGA/DSC) techniques. In addition, the antibacterial properties of the prepared POSS-CTX conjugate tested with the broth microdilution methods on *E.coli* and *S.aureus* bacteria. The cytotoxicity of the conjugate was detected in the in vitro cell culture system with the MTT test on L929 mouse skin fibroblast cells.

2. Experimental

2.1. Materials

The chemicals were purchased from Sigma-Aldrich. The Dimethyl sulfoxide (DMSO) was obtained from Carlo Erba. The 3-(4,5-dimethylthiazol-2-yl)-2,5-diphenyltetrazolium bromide (MTT) was purchased from AppliChem. Fetal Bovine Serum (FBS) (Biowest), Penicillin-Streptomycin (PAN Biotech), Dulbecco's Modified Eagle Medium (DMEM) (Capricorn Scientific). The mouse skin fibroblast cell line (L929) was sub-cultured from a stock culture obtained from the Hacettepe University Faculty of Science. Müller Hinton Agar and Müller Hinton Broth (Or-Bak). In the antibacterial studies were used *Escherichia coli* (*E.coli*) ATCC: 25922 and *Staphylococcus aureus* (*S.aureus*) ATCC: 29213 bacteria. These bacteria were supplied from the medical faculty at Inonu University.

2.2. Synthesis of the octakis(3-chloropropyl)octasilsesquioxane (POSS-Cl)

The octakis(3-chloropropyl)octasilsesquioxane (POSS-Cl) was synthesized from 3-chloropropyltrimethoxysilane by the sol-gel method. 3-chloropropyltrimethoxysilane (45 ml) was added to 100 ml of dry methanol. The concentrated HCl (28 ml) was added to this mixture and stirred for two days at room temperature. $PtCl_4$ (5 mmol) was added to this solution as catalyst in an argon atmosphere. The reaction mixture was heated to 50 °C and the mixture was cooled to room temperature. The white crystalline product was obtained (Demirel et al., 2014).

2.3. Synthesis of polyhedral oligomeric silsesquioxane-cefotaxime (POSS-CTX) conjugate

The POSS-CTX conjugate was prepared from octakis(3-chloropropyl) octasilsesquioxane and cefotaxime. In a typical synthesis, the POSS-Cl and cefotaxime as a stoichiometric ratio (1/8 mmol) were dissolved in 15 ml DMSO and poured into a glass flask. The reaction solution was deoxygenated by bubbling N_2 gas at room temperature for 30 min, and was then heated to 70 °C with a stirring for 1.5 h, followed by the addition of 0.01 g potassium carbonate. The reaction was continued for 4 h at 70 °C, and the mixture was then cooled to 50 °C. The obtained POSS-CTX structure was washed several times with ethanol and dried at 50 °C for 12 h.

2.4. Antibacterial activity

The antibacterial activity was evaluated by the determination of IC₅₀ using the broth microdilution methods against *Escherichia coli* (*E.coli*) ATCC: 25922, *Staphylococcus aureus* (*S.aureus*) ATCC: 29213. The experimental stage can be listed in five steps. Firstly; chloro-functional POSS, cefotaxime and POSS-cefotaxime conjugate were prepared in 10000 µg/mL stock solution. Secondly; the selection of colonies. Thirdly; the set of bacterial suspension used in the assay was performed according to 0.5 McFarland (0.5 McFarland standard is prepared by mixing 0.05 mL of 1.175 % $BaCl_2 \cdot 2H_2O$ with 9.95 mL of 1% sulfuric acid H_2SO_4). After this, the broth microdilution method was used in 96-well plates. The plates were incubated at 37°C for 18-24 h. Finally; the samples were taken from the well plates cultivated by using the MHB agar, and then were incubated for 18-24 h 37°C. After the counting process was performed, the IC₅₀ values were calculated (Luber et al., 2003, Kidwai et al., 2005, Polcyn et al., 2009).

2.5. Evaluation of cytotoxicity with MTT assay

MTT assay; measuring the cytotoxicity depending on cell viability is often used via an easy and comfortable colorimetric method (Ferrari et al., 1990, Chen et al., 2014). This method is reduced by metabolically active cells; in part by the action of dehydrogenase enzymes (Jo et al., 2015, Mitrovic et al., 1994). The L929 mouse skin fibroblast cells with 10% FBS and 1% penicillin/streptomycin in DMEM medium cultured at 37°C incubator containing 5% CO_2 . Density of 5000 cells were cultured in 96-well plates and incubated for 24 hours in the same conditions. The samples were prepared from stock solutions of 200, 100, 50, 25, 10 µM concentration diluted with DMEM medium. 96-well plates attached to the medium of the cells were replaced in a sample solution. The control wells were replaced with a fresh medium. The medium was removed and the wells were added respectively 90 µL DMEM and 10

μL MTT (5mg/mL, in PBS). The same conditions were incubated in the dark for 4 hours and then after removing the solution 100 μL DMSO was added. The absorbance measurements were performed by using a microplate reader at 540 nm. The value of the sample of % living cells was detected based on the absorbance results.

2.6. Statistical analysis

The statistical analyses were performed with Graphpad Prism 5 software. All the data was presented as mean values \pm standart deviation.

3. Results and Discussion

3.1. Structural characterization of POSS-Cl, CTX and POSS-CTX

The POSS-Cl, CTX, and POSS-CTX conjugate were characterized by FTIR, ^1H NMR, DTA, TGA, DSC, SEM/EDX. Fig. 1 shows the FTIR spectra of CTX, POSS-Cl, and POSS-CTX. The main characteristic peaks of the pure CTX appeared at 1050 cm^{-1} (etheral C-O), 1276 cm^{-1} (etheral C-O-C), 1302 cm^{-1} (C-S-C), 1342 cm^{-1} (on the thiazole ring stretching vibration of the C-S=C bond), 1440 cm^{-1} (C-N), 1590 cm^{-1} (N-H), 1600 cm^{-1} (amide C=O), 1770 cm^{-1} (sodium atom C=O), 1820 cm^{-1} (esteric C=O), $2850\text{-}2946\text{ cm}^{-1}$ (aliphatic C-H stretching vibrations), 3294 cm^{-1} (in thiazole $\text{NH}_2\text{-C}$ vibration). For the POSS-Cl structure, a Si-O stretching peak at 655 cm^{-1} , a strong Si-O-Si band at 1115 cm^{-1} , and aliphatic C-H stretching peaks at $2800\text{-}2914\text{ cm}^{-1}$ were observed. For the POSS-CTX, the characteristic peaks of both POSS and CTX groups appeared at 952 cm^{-1} (aliphatic C-H), 1033 cm^{-1} (Si-O), 1115 cm^{-1} (Si-O-Si), 1367 cm^{-1} (C-N), 1533 cm^{-1} (C=C), 1614 cm^{-1} (C=O), 2937 cm^{-1} (C-H stretching). 3294 cm^{-1} $\text{NH}_2\text{-C}$ stretching in cefotaxime disappearance also proved to us that the desired structure was obtained (Gültek et al., 2005, Mahmoud et al., 2015).

The structural characterization of the POSS-Cl, CTX, and POSS-CTX conjugate was also made by ^1H NMR (Fig. 2, 3, 4). For POSS-Cl ^1H NMR (DMSO, d^6): 3.64 (t, $\text{Si-CH}_2\text{CH}_2\text{Cl}$, 16H); 1.84 (m, SiCH_2CH_2 , 16H); 0.81 (t, SiCH_2 , 16H). For CTX ^1H NMR (DMSO, d^6): 7.27 ppm (aromatic C-H proton); 5.62 ppm (N-H proton) and 5.01 ppm (NH_2 proton); 3.84 ppm (aliphatic $\text{CH}_3\text{-O}$ proton); 3.19 and 3.51 ppm (aliphatic CH_2 proton); 2.01 ppm (esteric - CH_3 proton). For POSS-CTX ^1H NMR (DMSO, d^6): 7.19 ppm (aromatic C-H proton); 3.84 ppm (O- CH_3 proton); 2.99 ppm (CH_2N proton); 2.01 (m, SiCH_2CH_2 , 16H); 1.23 (t, SiCH_2 , 16H). In here, the 2.99 ppm proton of the CH_2N group is seen which is a sign of binding.

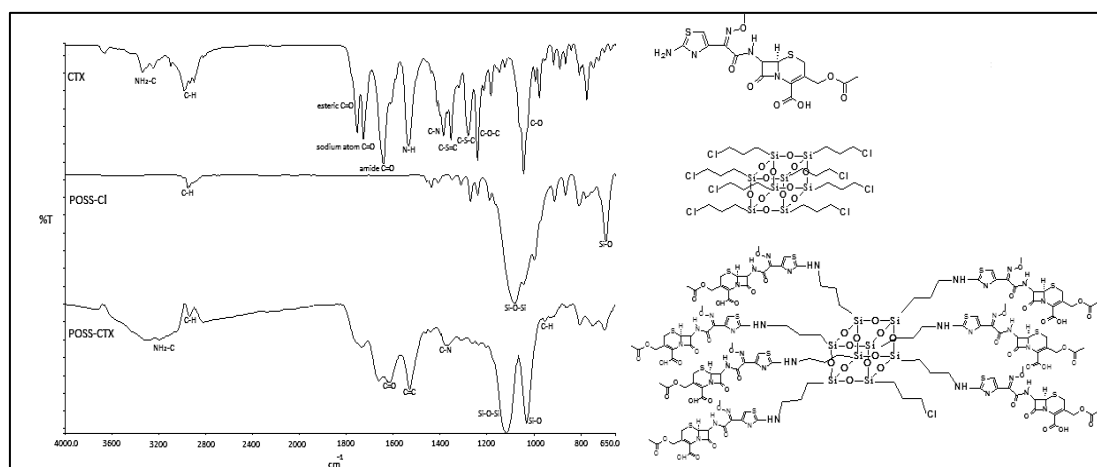


Fig 1. FTIR spectra of CTX, POSS-Cl and POSS-CTX.

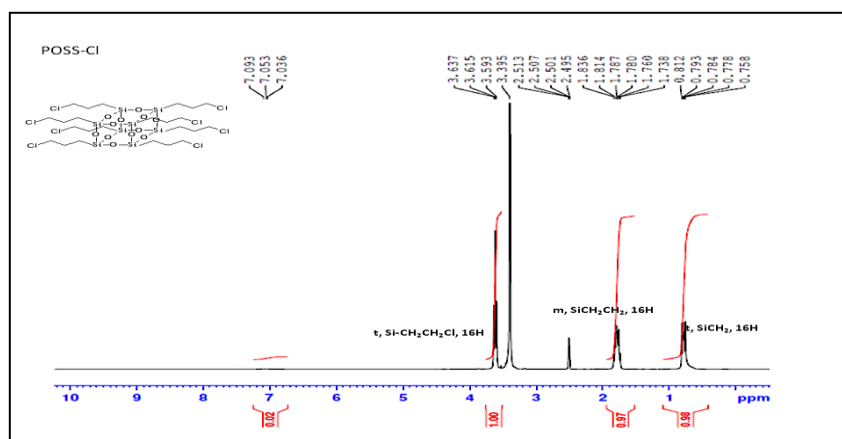


Fig 2. ¹H NMR spectra of POSS-Cl.

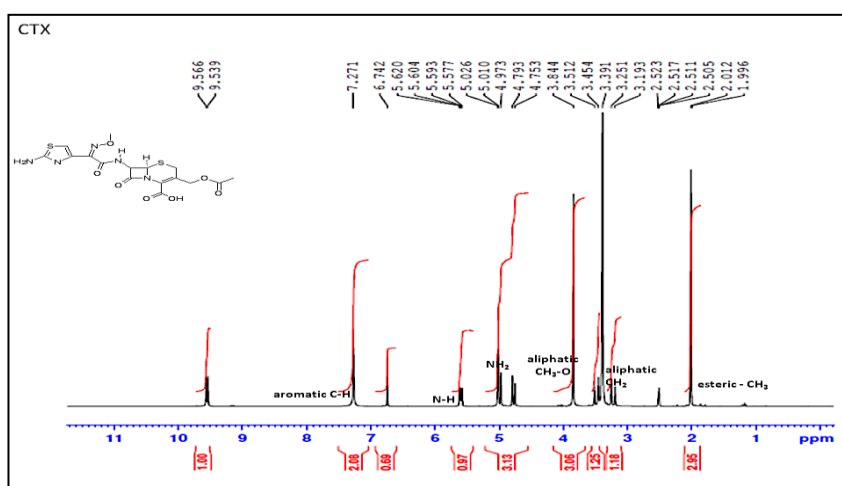


Fig 3. ¹H NMR spectra of CTX.

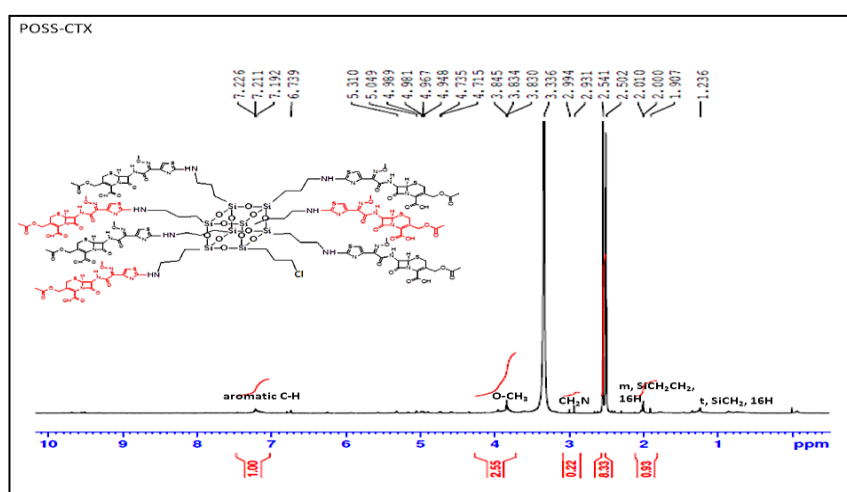


Fig 4. ¹H NMR spectra of POSS-CTX.

3.2. Thermal analysis of POSS-Cl, CTX and POSS-CTX

The thermal analysis results were obtained with TGA, DTA, and DSC techniques. The TGA, DTA, and DSC results are given respectively in Fig. 5, Fig. 6 and Fig. 7. The POSS-Cl showed high thermal stability and it could be seen that the thermal resistance rose to 326 °C. The organic side groups on the POSS-Cl structure degrade after the value of the temperature. The total mass loss value was about 50 % at 700 °C. The gradual degradation of the cefotaxime group was observed in the temperature areas. We saw that the humidity out of the building was at 100 °C. In the TGA thermograms of POSS-CTX; the

moisture away from the building was at 110 °C. General molecular structure is thermally stable up to 220 °C. We see that the increase of the thermal stability of cefotaxime structure connecting the POSS group. DTA thermograms for POSS-Cl, CTX and POSS-CTX are given in Fig. 6. In these curves, we see the crystallization of pure POSS structure of the transition around 200 °C. It is also observed that there is a deteriorating organic structure of 350-565 °C. Cefotaxime structure shows three basic mass loss between 200-310 °C, 310-485 °C and 485-655 °C. The first mass loss which is due to degradation of the aliphatic side group structure CH_2CH_3 . The second mass loss was caused in the five-membered ring degradation. The last mass loss was caused as a result of the thermal degradation of the bridged rings. Finally, a simple thermal decomposition peak between 650-700 °C was observed. The decomposition peak of the cefotaxime ester side groups was observed at 210-320°C. The five membered ring decay was observed at 320-450°C. The basic bridged ring decomposition band was observed at 530-680°C. The thermal behaviors of POSS-Cl, CTX, and POSS-CTX were also investigated by DSC analysis, and the results matched with the DTA analysis. In DSC thermograms of the POSS-Cl structure, the POSS structure had no significant degradation at the 30-400°C temperature range, but in the DSC thermogram of the pure cefotaxime, the main thermal decomposition peak was shown at 198°C. However, the decomposition temperature of the POSS-Cefotaxime structure began at 250°C. Through the DSC thermograms, it can be concluded from these results that the binding of the molecule increases the thermal stability of the cefotaxime.

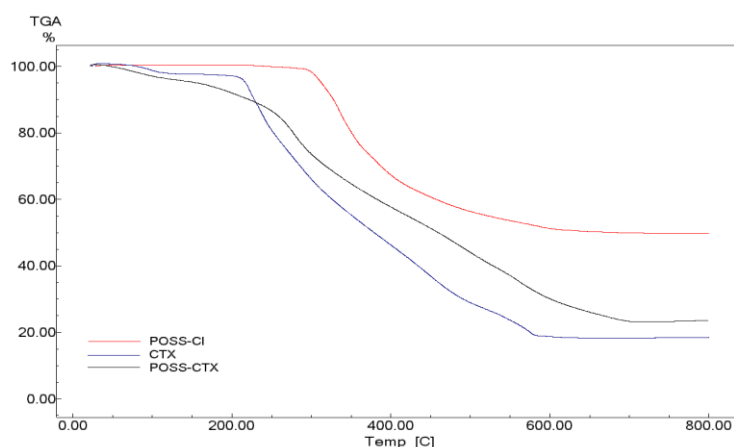


Fig 5. TGA thermograms of POSS-Cl, CTX and POSS-CTX

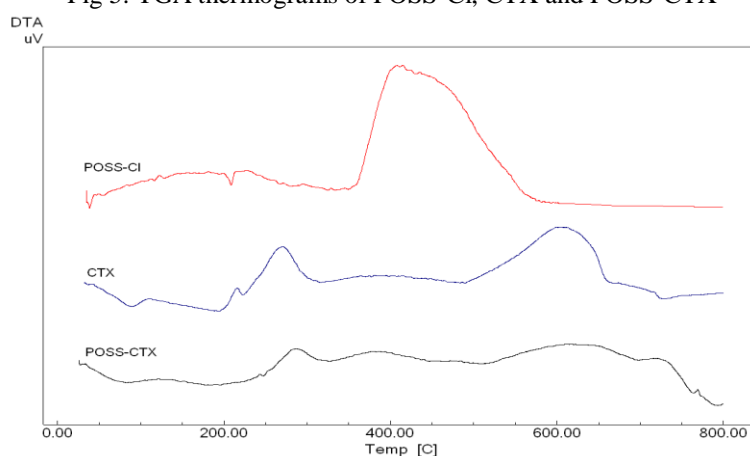


Fig 6. DTA thermograms of POSS-Cl, CTX and POSS-CTX

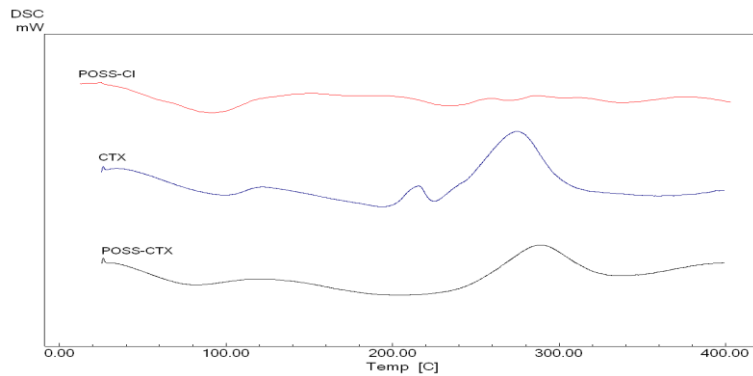


Fig 7. DSC thermograms of POSS-Cl, CTX and POSS-CTX

3.3. Surface analysis of POSS-Cl, CTX, and POSS-CTX

The SEM images of the structures POSS-Cl, pure CTX, and POSS-CTX conjugate are given comparatively in low and high magnification in Fig. 8. Compared with the starting materials (POSS and pure CTX), the SEM images of the resulting POSS-CTX conjugate observed are quite different and homogenous. The SEM images of the POSS structure exhibit a fractal structure. Quite large surface cavities show the high-magnification in the SEM. The SEM images of the pure CTX are shown in small parts in the structure. These parts seemed to consist of the broken plane in high-magnification. In the POSS-CTX structure, the surface was dominated by a homogeneous powder form. The planary parts were destroyed and formed small cavities. The structural differentiation proves the formation of a new structure. The homogenous appearance shows the purity of the product. The EDX spectra of the POSS-Cl, CTX, and POSS-CTX conjugate can be seen in Fig. 9. The C, O, Cl, and Si peaks can be seen clearly in the spectrum of the POSS-Cl structure. We can see in the spectral maps the C (0.277 keV), O (0.523 keV), Si (1.743 keV), and Cl (2.622 keV) peaks. The pure cefotaxime structure convenience was in the S, N, C, Na, and O elements. We can see this in the spectral maps C (0.277 keV), O (0.523 keV), S (2.307 and 0.149 keV), and Na (1.040 keV) peaks. The peaks originated from both the POSS and CTX molecules seen in the POSS-CTX structure. We could see clearly that C (0,277 keV), O (0,523 keV), S (2,307 and 0,149 keV), Si (1,743), Na(1,040 keV) peaks. These results seem to confirm that the desired POSS-CTX structure was obtained to a large extent. Also, the EDX elemental mapping image also shows the homogeneity of the final product structure.

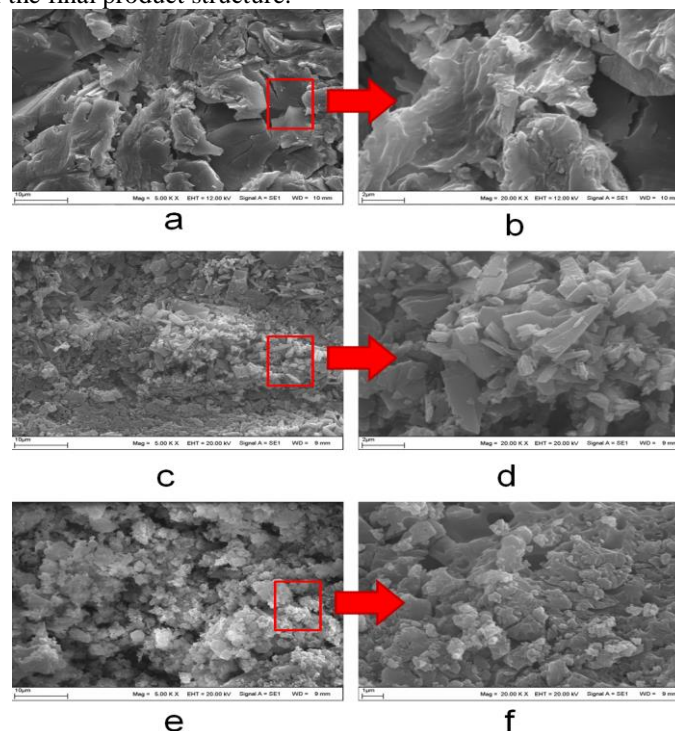


Fig 8. (a, b) SEM images of POSS-Cl. (c, d) SEM images of CTX. (e, f) SEM images of POSS-CTX conjugate.

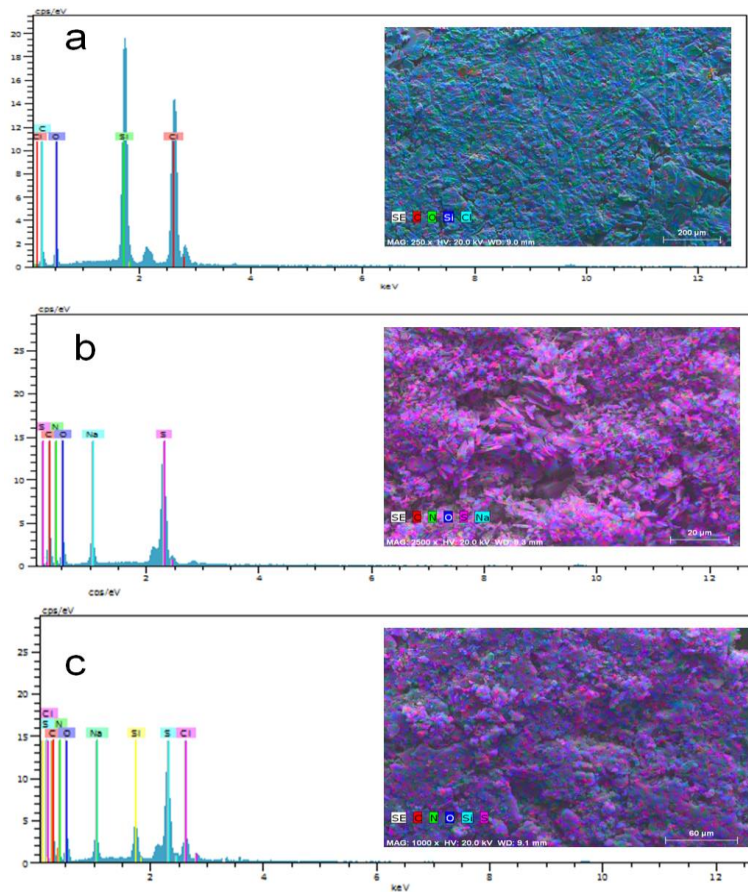


Fig 9. (a) EDX elemental mapping images for POSS-Cl. (b) EDX elemental mapping images for CTX. (c) EDX elemental mapping images for POSS-CTX conjugate.

3.4. Antibacterial activity results

The antibacterial activity was tested against Gram negative (*E.coli*) and Gram positive (*S.aureus*) bacteria. It was determined according to the broth microdilution method. The IC₅₀ values were calculated for only antibacterial activity CTX and POSS-CTX and were given in Fig. 10. According to our results; the antibacterial activity for POSS-Cl was not determined for *E.coli* and *S.aureus*. These observations are given in Fig. 11. The IC₅₀ values of CTX were found as $62.71 \pm 14.30 \mu\text{g/mL}$ for *E.coli* and $144.17 \pm 20.90 \mu\text{g/mL}$ for *S.aureus*. However, the IC₅₀ values of the POSS-CTX conjugate were measured as 11.51 ± 3.02 and $26.20 \pm 11.14 \mu\text{g/mL}$ for *E.coli* and *S.aureus*, respectively. The IC₅₀ values revealed that the POSS-CTX conjugate is a more effective antibacterial agent when compared with pure CTX.

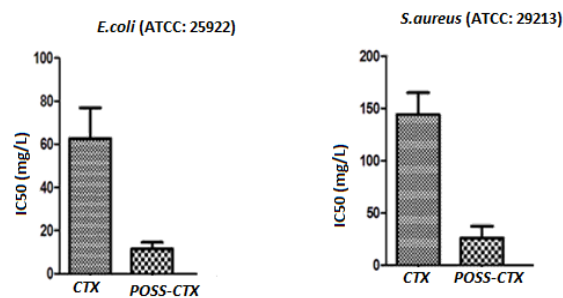


Fig 10. IC₅₀ values for CTX and POSS-CTX conjugate.

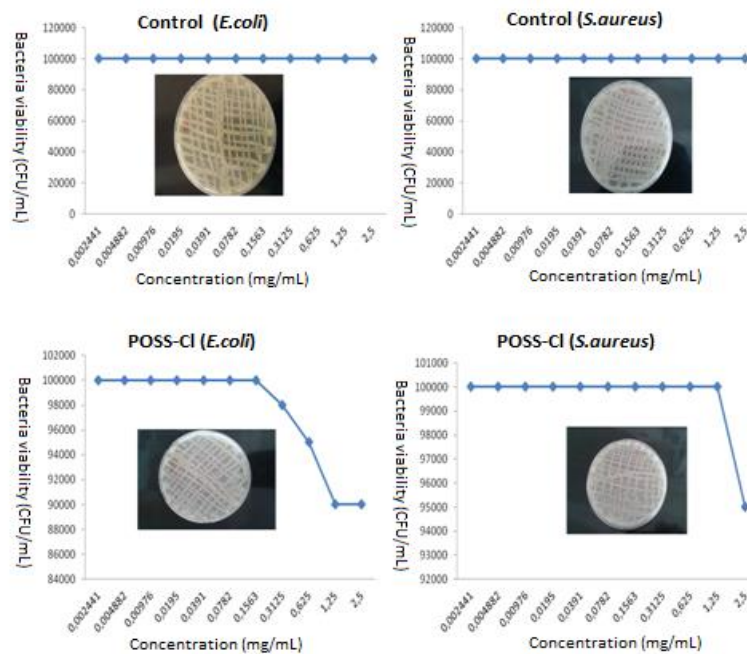


Fig 11. Bacteria viability-concentration relationship for control and POSS-Cl.

3.5. Cell culture cytotoxicity results

Cytotoxicity results were successfully performed on L929 mouse skin fibroblast cells. The cytotoxicity results and cell images are shown in Fig. 12. POSS-CTX conjugate was experimentally proven with non cytotoxic on L929 cells in a lower concentration from 200 μ M. According to ISO-10993-5, the inhibition of cell viability by more than 30% is considered as a cytotoxic effect for biomaterials. The POSS-CTX conjugate exhibited high cell viability (>90%) in a range from 25 to 200 μ M (Fig. 12). These results were also evaluated as Grade 1 according to ISO standards. Therefore, a synthesized POSS-CTX conjugate can be assumed nontoxic.

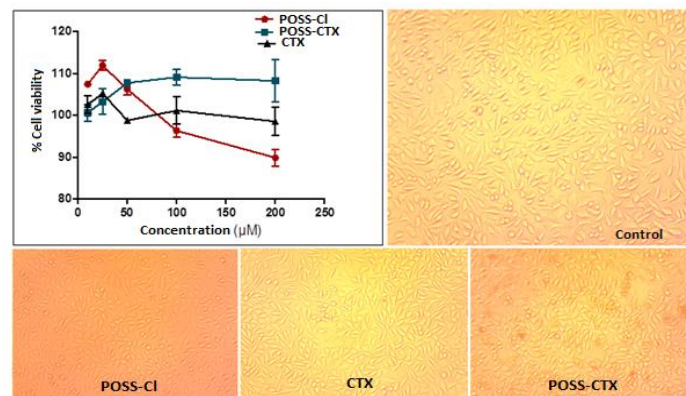


Fig 12. Cell viability results and images for CTX and POSS-CTX conjugate.

4. Conclusions

As a result, we saw that there was a statistically significant increase in antibacterial activities in novel polyhedral oligomeric silsesquioxane-cefotaxime (POSS-CTX) according to cefotaxime (CTX) in *E.coli* ($p < 0.05$) and *S.aureus* ($p < 0.01$) in the same concentration. In addition, the POSS-CTX conjugate showed high cell viability, (almost ~100%) in the in vitro cell cytotoxicity test. This conjugate exhibited high antibacterial activity and good biocompatibility. The results of this research will provide a positive contributions many areas such as medical materials, antibacterial coating and antibacterial packaging.

References

- Chen, F., Wu, T., Cheng, X. (2014). Cytotoxic effects of denture adhesives on primary human oral keratinocytes, fibroblasts and permanent L929 cell lines. *Gerodontology*. 31: 4-10.

- Cordes, D.B., Lickiss, P.D., Rataboul, F. (2010). Recent developments in the chemistry of cubic polyhedral oligosilsesquioxanes. *Chem. Rev.* 110: 2081-2173.
- Demirel, M.H., Köytepe, S., Gültek, A., Seçkin, T. (2014). Synthesis and stimuli-responsive properties of the phenanthroline based metallo-supra molecular polymers. *J Polym Res.* 21: 345.
- Fakhri, A., Rashidi, S., Asif, M., Tyagi, I., Agarwal, S., Gupta, V.K. (2016). Dynamic adsorption behavior and mechanism of Cefotaxime, Cefradine and Cefazolin antibiotics on CdS-MWCNT nanocomposites. *J. Mol. Liq.* 215: 269-275.
- Ferrari, M., Fornasiero, M.C., Isetta, A.M. (1990). MTT colorimetric assay for testing macrophage cytotoxic activity in vitro. *J. Immunol. Methods.* 131: 165-172.
- Fong, H., Dickens, S.H. Flaim, G.M. (2005). Evaluation of dental restorative composites containing polyhedral oligomeric silsesquioxane methacrylate. *Dental Materials.* 21: 520-529.
- Ghanbari, H., Kidane, A.G., Burriesci, G., Ramesh, B., Darbyshire, A., Seifalian, A.M. (2010). The anti-calcification potential of a silsesquioxane nanocomposite polymer under in vitro conditions: Potential material for synthetic leaflet heart valve. *Acta Biomaterialia.* 6: 4249-4260.
- Gültek, A., Seçkin, T., Adıgüzel, H.İ. (2005). Design and characterization of amino and chloro functionalized rhombohedral silsesquioxanes. *Turk J Chem.* 29: 391-399.
- Huang, C., Wei, Z., Zhang, L., Luo, X., Ren, H., Luo, M. (2013). Preparation and characterization of polyhedral oligomeric silsesquioxane–titania aerogels. *J. Porous Mater.* 20: 1017-1022.
- Jo, H.Y., Kim, Y., Park, H.W., Moon, H.E., Bae, S., Kim, J.W., Kim, D.G., Paek S.H. (2015). The Unreliability of MTT Assay in the Cytotoxic Test of Primary Cultured Glioblastoma Cells. *Exp.Neurobiol.* 24: 235-245.
- Kidwai, M., Saxena, S., Khan, M.K.R., Thukral, S.S. (2005). Aqua mediated synthesis of substituted 2-amino-4H-chromenes and in vitro study as antibacterial agents. *Bioorg. Med. Chem. Lett.* 15: 4295-4298.
- Li, G.Z., Wang, H.N., Pittman, C.U. (2001). Polyhedral oligomeric silsesquioxane (POSS) polymers and copolymers. *J. Inorg. Organomet. Polym.* 11: 123-154.
- Li, G.Z., Yamamoto, T., Nozaki, K., Hikosaka, M. (2009). Crystallization of ladder like polyphenyl silsesquioxane (PPSQ)/isotactic polystyrene (i-PS) blends. *Polymer.* 42: 8435-8441.
- Liang, K., Toghian, H., Li, G., Pittman, C.U. (2005). Synthesis, morphology, and viscoelastic properties of cyanate ester/polyhedral oligomeric silsesquioxane nanocomposites. *J. Polym. Sci.* 43: 3887-3898.
- Luber, P., Bartelt, E., Genschow, E., Wagner, J., Hahn, H. (2003). Comparison of Broth Microdilution, E Test, and Agar Dilution Methods for Antibiotic Susceptibility Testing of *Campylobacter jejuni* and *Campylobacter coli*. *Exp Neurobiol.* 24: 235-245.
- Mahmoud, M.A., Akmal, S.G., Said, M.T. (2015). Spectroscopic and thermal investigation of charge-transfer complexes formed between cefotaxime sodium drug and various acceptors. *Russ J Gen Chem.* 85:731-745.
- Masuyashi, S., Arai, S., Miyamoto, M., Mitsuhashi, S. (1980). InVitro Antimicrobial Activity of Cefotaxime, a New Cephalosporin. *Antimicrob. Agents Chemother.* 18: 1-8.

- McCusker, C., Carrol, J.B., Rotello, V.M. (2005). Cationic polyhedral oligomeric silsesquioxane (POSS) units as carriers for drug delivery processes. *Chem. Commun.* 8: 996-998.
- Mitrovic, B., Ignarro, L.J., Montestrucque, S., Small, A., Merril, J.E. (1994). Nitric oxide as a potential pathological mechanism in demyelination : its differential effects on primary glial cells in vitro. *Neuroscience.* 61: 575-585.
- Polcyn, P., Jurczak, M., Rajnisz, A., Solecka, J., Urbanczyk-Lipkourska, Z. (2009). Design of Antimicrobially Active Small Amphiphilic Peptide Dendrimers. *Molecules.* 14: 3881-3905.
- Sarkar, S., Buriesci, G., Wojcik, A., Aresti, N., Hamilton, G., Seifalian, A.M. (2009). Manufacture of small calibre quadruple lamina vascular bypass grafts using a novel automated extrusion-phase-inversion method and nanocomposite polymer. *J Biomech.* 42: 722-730.
- Türkeş, C., Söyüt, H., Beydemir, Ş. (2015). Human serum paraoxonase-1 (hPON1): *in vitro* inhibition effects of moxifloxacin hydrochloride, levofloxacin hemihidrate, cefepime hydrochloride, cefotaxime sodium and ceftizoxime sodium. *J. Enzyme Inhib. Med. Chem.* 30: 622-628.
- Zou, Q.C., Yan, Q.J. Song, G.W. Zhang, S.L. Wu, L.M. (2007). Detection of DNA using cationic polyhedral oligomeric silsesquioxane nanoparticles as the probe by resonance light scattering technique. *Biosensors and Bioelectronics.* 22: 1461-1465.